



HAL
open science

Returns to the origin of the Pólya walk with stochastic resetting

Claude Godrèche, Jean-Marc Luck

► **To cite this version:**

Claude Godrèche, Jean-Marc Luck. Returns to the origin of the Pólya walk with stochastic resetting. 2023. cea-04265008

HAL Id: cea-04265008

<https://cea.hal.science/cea-04265008>

Preprint submitted on 30 Oct 2023

HAL is a multi-disciplinary open access archive for the deposit and dissemination of scientific research documents, whether they are published or not. The documents may come from teaching and research institutions in France or abroad, or from public or private research centers.

L'archive ouverte pluridisciplinaire **HAL**, est destinée au dépôt et à la diffusion de documents scientifiques de niveau recherche, publiés ou non, émanant des établissements d'enseignement et de recherche français ou étrangers, des laboratoires publics ou privés.

Returns to the origin of the Pólya walk with stochastic resetting

Claude Godrèche and Jean-Marc Luck*

Université Paris-Saclay, CEA, CNRS, Institut de Physique Théorique,
91191 Gif-sur-Yvette, France.

*Corresponding author(s). E-mail(s): jean-marc.luck@ipht.fr;
Contributing authors: claude.godreche@ipht.fr;

Abstract

We consider the simple random walk (or Pólya walk) on the one-dimensional lattice subject to stochastic resetting to the origin with probability r at each time step. The focus is on the joint statistics of the numbers \mathcal{N}_t^\times of spontaneous returns of the walker to the origin and \mathcal{N}_t^\bullet of resetting events up to some observation time t . These numbers are extensive in time in a strong sense: all their joint cumulants grow linearly in t , with explicitly computable amplitudes, and their fluctuations are described by a smooth bivariate large deviation function. A non-trivial crossover phenomenon takes place in the regime of weak resetting and late times. Remarkably, the time intervals between spontaneous returns to the origin of the reset random walk form a renewal process described in terms of a single ‘dressed’ probability distribution. These time intervals are probabilistic copies of the first one, the ‘dressed’ first-passage time. The present work follows a broader study, covered in a companion paper, on general nested renewal processes.

1 Introduction

This work builds upon a previous study on the replication of a renewal process at random times, which is equivalent to nesting two generic renewal processes, or, alternatively, to considering a renewal process subject to random resetting [1]. In that study, we investigated the interplay between the two probability laws governing the distribution of time intervals between renewals, on the one hand, and resettings, on the other hand, resulting in a phase diagram that highlights a rich range of behaviours.

In the present work, we investigate the specific case where the internal renewal process consists of the epochs of returns to the origin of the simple random walk (or Pólya walk [2]) on the one-dimensional lattice, while the external one involves discrete-time reset events at which the process is restarted from the origin with probability r at each time step. The position x_t of the walker at discrete time t thus obeys the recursion

$$x_{t+1} = \begin{cases} 0 & \text{with probability } r, \\ x_t + \eta_{t+1} & \text{with probability } 1 - r, \end{cases} \quad (1.1)$$

where $\eta_t = \pm 1$ with equal probabilities. The walk starts at the origin, $x_0 = 0$. Figure 1 illustrates a sample path of the walk, showing spontaneous returns to the origin marked by crosses and reset events marked by dots. Figure 2 provides a depiction of these temporal events and of the intervals of time between them.

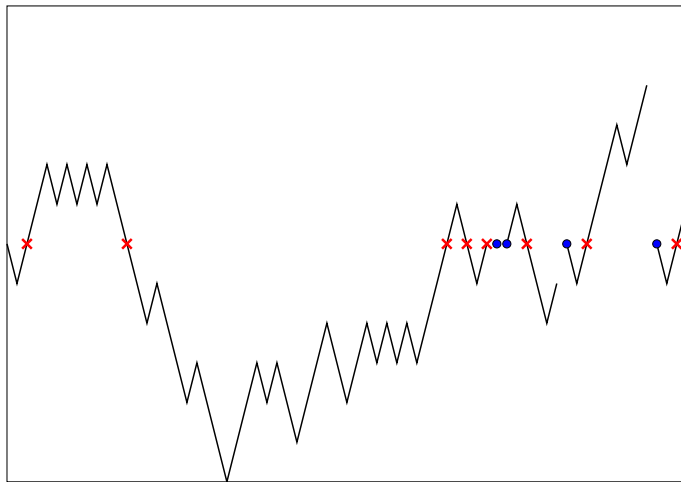


Fig. 1 Example of a path of the Pólya walk on the one-dimensional lattice under stochastic resetting, generated by a simulation with $r = 0.08$. The walk starts at the origin. It restarts afresh at the origin at each resetting event, figured by a dot. Spontaneous returns to the origin are figured by crosses.

Much of the research in the theory of resetting processes has predominantly concentrated on continuous time stochastic processes (see [3] for a review). In contrast, relatively less emphasis has been devoted to discrete-time processes. An illustrative example of these processes involves discrete-time random walks with continuous distributions of steps subject to resetting [4]. Recent studies have delved into the statistics of extremes and records of symmetric random walks with stochastic resetting [5, 6]. Furthermore, investigations into discrete-time lattice random walks with resetting have also been carried out. Examples include unidirectional random walks with random restarts [7], random walks where the walker is relocated to the previous maximum [8], and random walks with preferential relocations to previously visited locations [9].

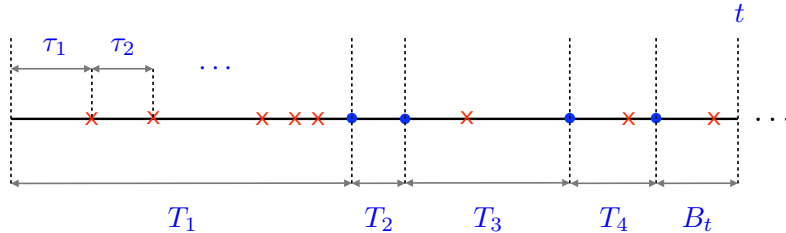


Fig. 2 Sketch of the temporal events for the path of figure 1. Spontaneous returns to the origin of the walk are figured by crosses, resetting events by dots. The intervals of time between two crosses, τ_1, τ_2, \dots , have common distribution $\rho(\tau)$ (see (2.1), (2.2)). The intervals of time between two resettings, T_1, \dots, T_4 , have the geometric distribution (2.32). The last interval, B_t , represents the backward recurrence time, or age of the resetting process at time t , i.e., the time elapsed since the previous resetting event.

However, it is noteworthy that the Pólya walk subject to resetting, defined by (1.1), has received relatively limited attention in the literature [6, 10–13]. References [10, 11] deal with general first-passage properties of lattice random walks in discrete time, with application to the Pólya walk, while [12] contains a study of some aspects of the statistics of records for the same walk. In [13], an analysis of the survival probability of symmetric random walks with stochastic resetting was performed, specifically focussing on the probability for the walker not to cross the origin up to time t , including the example of the Pólya walk (1.1). Finally, the statistics of extremes and records for the Pólya walk with stochastic resetting are discussed in [6].

The focus of the present work is on the joint statistics of the numbers \mathcal{N}_t^\times of spontaneous returns to the origin of the reset Pólya walk (1.1), and \mathcal{N}_t^\bullet , denoting the count of reset events, up to a given time t . These are the simplest observables one can think of for this process. Their sum $\mathcal{N}_t^{\times\bullet} = \mathcal{N}_t^\times + \mathcal{N}_t^\bullet$ is the total time spent by the walker at the origin.

The motivation for such a research stems from the analysis presented in the companion paper [1]. The latter predicts that the more regular of two nested renewal processes always governs the overall regularity of the entire process. Here, the two renewal processes in question are made of the sequence of spontaneous returns to the origin of the Pólya walk, on the one hand, and of the sequence of resetting events, on the other hand. The latter—the more regular process of the two—is a Bernoulli process, as can be seen on its definition (1.1). In such a circumstance, as demonstrated in [1], $\langle \mathcal{N}_t^\times \rangle$ grows linearly in time and typical fluctuations of \mathcal{N}_t^\times around its mean value are relatively negligible. The purpose of the present work is to corroborate these general results and complete them by a thorough quantitative analysis of the simple specific case at hand—the Pólya walk under stochastic resetting.

The setup and the main outcomes of this research are as follows. Section 2 gives an exposition of background concepts and results. For the Pólya walk without resetting (section 2.1), we recall results concerning the distribution of the intervals between consecutive returns to the origin, and the statistics of the number N_t of such returns up to some time t . Section 2.2 contains a reminder on the statistics of resetting events in discrete time. Section 3 presents the detailed derivation of the joint probability

generating function of the random variables \mathcal{N}_t^\times and \mathcal{N}_t^\bullet at any finite time t . As a first application of the key equation (3.20), derived in section 3.1, the mean values of \mathcal{N}_t^\times and \mathcal{N}_t^\bullet are shown to grow linearly in time, as

$$\langle \mathcal{N}_t^\times \rangle \approx A^\times t, \quad \langle \mathcal{N}_t^\bullet \rangle \approx rt, \quad \langle \mathcal{N}_t^{\times\bullet} \rangle \approx At, \quad (1.2)$$

where the amplitude

$$A = A^\times + r = \sqrt{\frac{r}{2-r}} \quad (1.3)$$

is identified with the steady-state probability for the walker to be at the origin. In addition, we give in section 3.2 an interpretation of the distribution of \mathcal{N}_t^\times in terms of a single ‘dressed’ renewal process, and discuss its consequences. An in-depth investigation of the statistics of \mathcal{N}_t^\times and \mathcal{N}_t^\bullet in the late-time regime is done in section 4, highlighting the fact that these quantities are extensive in a strong sense: their joint cumulants grow linearly in time, as

$$\langle (\mathcal{N}_t^\times)^k (\mathcal{N}_t^\bullet)^\ell \rangle_c \approx c_{k,\ell} t. \quad (1.4)$$

We provide a method to evaluate all the cumulant amplitudes $c_{k,\ell}$, and we give the explicit expressions of the first amplitudes corresponding to $k + \ell \leq 3$ (see (4.13)–(4.15)). The above scaling law of cumulants is virtually equivalent to the statement that large fluctuations of \mathcal{N}_t^\times and \mathcal{N}_t^\bullet far from their mean values obey a large deviation formula of the form

$$\mathbb{P}(\mathcal{N}_t^\times \approx \xi t, \mathcal{N}_t^\bullet \approx \eta t) \sim e^{-I(\xi,\eta)t}, \quad (1.5)$$

where the bivariate large deviation function $I(\xi,\eta)$ is the Legendre transform of the bivariate entropy function $S(\lambda,\mu)$ generating the cumulant amplitudes $c_{k,\ell}$. The ensuing univariate large deviation functions $I^\bullet(\eta)$, $I^\times(\xi)$, and $I(\varphi)$, corresponding respectively to \mathcal{N}_t^\bullet , \mathcal{N}_t^\times and their sum $\mathcal{N}_t^{\times\bullet}$, are plotted in figure 7. In the crossover regime at weak resetting and late times, studied in section 5, it is found that

$$\mathcal{N}_t^\times \approx \sqrt{t} \zeta, \quad (1.6)$$

where the rescaled random variable ζ has a limiting distribution with density $f(\zeta, u)$, depending solely on the parameter $u = rt = \langle \mathcal{N}_t^\bullet \rangle$. Figure 8 shows the density $f(\zeta, u)$ for several values of this parameter, illustrating the crossover between a half-Gaussian form at $u = 0$ and a drifting Gaussian at large u . Section 6 contains a brief discussion, where the main outcomes of the present work are put in perspective with those of the companion paper [1]. Some calculation details pertaining to section 3 are relegated to an appendix.

2 Background concepts

2.1 Pólya walk without resetting

As is well documented (see, e.g., [14]), the sequence of returns to the origin of the Pólya walk forms a discrete renewal process. Let us denote by $\mathbf{T}_{0 \rightarrow 0}$ the time of first

return to the origin (from either side), and its distribution by

$$\rho(\tau) = \mathbb{P}(\mathbf{T}_{0 \rightarrow 0} = \tau). \quad (2.1)$$

This quantity is non-zero whenever $\tau = 2, 4, \dots$ is an even integer. This is also the common distribution of the intervals between two consecutive returns to the origin, denoted by τ_1, τ_2, \dots , which are independent copies of $\mathbf{T}_{0 \rightarrow 0}$. The distribution $\rho(\tau)$ is known in terms of its generating function [14]

$$\tilde{\rho}(z) = \sum_{\tau \geq 0} z^\tau \rho(\tau) = 1 - \sqrt{1 - z^2}. \quad (2.2)$$

Introducing the binomial probabilities

$$b_n = \frac{(2n)!}{(2^n n!)^2} = \frac{\binom{2n}{n}}{2^{2n}}, \quad (2.3)$$

with generating function

$$\tilde{b}(z) = \sum_{n \geq 0} b_n z^n = \frac{1}{\sqrt{1 - z}}, \quad (2.4)$$

we have

$$\rho(2n) = \frac{b_n}{2n - 1} \quad (2.5)$$

for $n \geq 1$, i.e.,

$$\rho(2) = \frac{1}{2}, \quad \rho(4) = \frac{1}{8}, \quad \rho(6) = \frac{1}{16}, \quad \rho(8) = \frac{5}{128}, \quad (2.6)$$

and so on. When the even time τ becomes large, we have

$$\rho(\tau) \approx \sqrt{\frac{2}{\pi \tau^3}}. \quad (2.7)$$

The corresponding survival probability, defined as the complementary distribution function of $\mathbf{T}_{0 \rightarrow 0}$,

$$R(\tau) = \mathbb{P}(\mathbf{T}_{0 \rightarrow 0} > \tau) = \sum_{j > \tau} \rho(j), \quad (2.8)$$

obeys $R(\tau - 1) - R(\tau) = \rho(\tau)$. Its generating function reads

$$\tilde{R}(z) = \sum_{\tau \geq 0} z^\tau R(\tau) = \frac{1 - \tilde{\rho}(z)}{1 - z} = \frac{1 + z}{\sqrt{1 - z^2}}. \quad (2.9)$$

We have therefore

$$R(2n) = R(2n + 1) = b_n, \quad (2.10)$$

i.e.,

$$R(0) = R(1) = 1, \quad R(2) = R(3) = \frac{1}{2}, \quad R(4) = R(5) = \frac{3}{8}, \quad (2.11)$$

and so on. When τ becomes large, irrespective of its parity, we have

$$R(\tau) \approx \sqrt{\frac{2}{\pi\tau}}. \quad (2.12)$$

The asymptotic estimate (2.7) is minus twice the derivative of (2.12), as it should be, because (2.7) only holds for even times τ .

We now focus on the distribution of the number N_t of returns of the walker to the origin up to time t . This random variable is defined by the condition

$$\tau_1 + \dots + \tau_{N_t} \leq t < \tau_1 + \dots + \tau_{N_t+1}, \quad (2.13)$$

hence the total time t is decomposed into

$$t = \tau_1 + \dots + \tau_{N_t} + b_t, \quad (2.14)$$

where the last interval, b_t , is the backward recurrence time, or the age of the renewal process at time t , i.e., the elapsed time since the last return to the origin. In the present discrete setting, $b_t = 0, 1, \dots, \tau_{N_t+1} - 1$.

A realisation of the set of random variables $\tau_1, \dots, \tau_{N_t}, b_t$, with $N_t = n$, denoted by

$$\tilde{\mathcal{C}} = \{\tau_1, \dots, \tau_n, b\}, \quad (2.15)$$

has weight

$$P(\tilde{\mathcal{C}}) = \rho(\tau_1) \dots \rho(\tau_n) R(b) \delta\left(\sum_{i=1}^n \tau_i + b, t\right), \quad (2.16)$$

where $\delta(i, j)$ is the Kronecker delta symbol.

The distribution of N_t ensues by summing the above weight over all variables $\{\tau_i\}$ and b :

$$p_n(t) = \mathbb{P}(N_t = n) = \sum_{\{\tau_i\}, b} \rho(\tau_1) \dots \rho(\tau_n) R(b) \delta\left(\sum_{i=1}^n \tau_i + b, t\right). \quad (2.17)$$

The expression thus obtained is a discrete convolution, which is easier to handle by taking its generating function with respect to t , which reads

$$\sum_{t \geq 0} w^t p_n(t) = \tilde{\rho}(w)^n \tilde{R}(w), \quad (2.18)$$

where $\tilde{\rho}(w)$ and $\tilde{R}(w)$ are respectively given by (2.2) and (2.9). The distribution of N_t can be expressed compactly through the probability generating function

$$Z(z, t) = \langle z^{N_t} \rangle = \sum_{n \geq 0} z^n p_n(t). \quad (2.19)$$

The generating function of the latter quantity with respect to t is

$$\tilde{Z}(z, w) = \sum_{t \geq 0} w^t Z(z, t) = \tilde{R}(w) \sum_{n \geq 0} (z \tilde{\rho}(w))^n, \quad (2.20)$$

i.e.,

$$\tilde{Z}(z, w) = \frac{1 - \tilde{\rho}(w)}{(1 - w)(1 - z \tilde{\rho}(w))}. \quad (2.21)$$

In particular, the generating function with respect to t of the mean number $\langle N_t \rangle$ of returns reads

$$\sum_{t \geq 0} w^t \langle N_t \rangle = \frac{\partial}{\partial z} \tilde{Z}(z, w) \Big|_{z=1} = \frac{\tilde{\rho}(w)}{(1 - w)(1 - \tilde{\rho}(w))} = \frac{1 + w}{(1 - w^2)^{3/2}} - \frac{1}{1 - w}. \quad (2.22)$$

We have therefore

$$\langle N_{2n} \rangle = \langle N_{2n+1} \rangle = (2n + 1)b_n - 1, \quad (2.23)$$

i.e.,

$$\langle N_0 \rangle = \langle N_1 \rangle = 0, \quad \langle N_2 \rangle = \langle N_3 \rangle = \frac{1}{2}, \quad \langle N_4 \rangle = \langle N_5 \rangle = \frac{7}{8}, \quad (2.24)$$

and so on. When time t becomes large, regardless of its parity, we have

$$\langle N_t \rangle \approx \sqrt{\frac{2t}{\pi}}. \quad (2.25)$$

The probability of having $N_t = 0$ is given by the generating function

$$\sum_{t \geq 0} w^t p_0(t) = \tilde{Z}(0, w) = \frac{1 - \tilde{\rho}(w)}{1 - w} = \tilde{R}(w) \quad (2.26)$$

(see (2.9)). We thus recover the expected result

$$p_0(t) = \mathbb{P}(\tau > t) = R(t). \quad (2.27)$$

The asymptotic distribution of N_t in the regime of late times can be extracted through a scaling analysis of (2.21). Setting $w = e^{-s}$ and $z = e^{-p}$, and working to leading order in the continuum regime where s and p are small, we obtain

$$\int_0^\infty dt e^{-st} \langle e^{-pN_t} \rangle \approx \frac{1}{s + p\sqrt{s/2}}. \quad (2.28)$$

Inverting the Laplace transforms in p and in s yields

$$\int_0^\infty dt e^{-st} p_n(t) \approx \sqrt{\frac{2}{s}} e^{-\sqrt{2s}n}, \quad (2.29)$$

and finally

$$p_n(t) \approx \sqrt{\frac{2}{\pi t}} e^{-n^2/(2t)}. \quad (2.30)$$

We have thus recovered the known property that the asymptotic distribution of the number N_t of returns to the origin of the simple random walk is a half-Gaussian [15]. The limit of this distribution as $n \rightarrow 0$ is consistent with the asymptotic behaviour of $R(t)$ given by (2.12). The moments of the distribution (2.30) read

$$\langle N_t^{2k} \rangle \approx \frac{(2k)!}{2^k k!} t^k, \quad \langle N_t^{2k+1} \rangle \approx \sqrt{\frac{2}{\pi}} 2^k k! t^{k+1/2}. \quad (2.31)$$

In particular, the first moment agrees with (2.25).

2.2 Statistics of resetting events

The resetting events also constitute a discrete renewal process, referred to in [1] as the external renewal process. The integer intervals of time $\mathbf{T}_1, \mathbf{T}_2 \dots$ between two consecutive resettings have the geometric distribution

$$f(T) = r(1-r)^{T-1} \quad (T \geq 1), \quad (2.32)$$

whose complementary distribution function is given by

$$\Phi(T) = \sum_{j>T} f(j) = (1-r)^T \quad (T \geq 0). \quad (2.33)$$

The corresponding generating functions read

$$\tilde{f}(z) = \sum_{T \geq 1} z^T f(T) = \frac{rz}{1 - (1-r)z}, \quad (2.34)$$

$$\tilde{\Phi}(z) = \sum_{T \geq 0} z^T \Phi(T) = \frac{1 - \tilde{f}(z)}{1 - z} = \frac{1}{1 - (1-r)z}. \quad (2.35)$$

The number of resetting events M_t is defined by the condition

$$\mathbf{T}_1 + \dots + \mathbf{T}_{M_t} \leq t < \mathbf{T}_1 + \dots + \mathbf{T}_{M_t+1}, \quad (2.36)$$

hence

$$t = \mathbf{T}_1 + \dots + \mathbf{T}_{M_t} + B_t, \quad B_t = 0, 1, \dots, \mathbf{T}_{M_t+1} - 1. \quad (2.37)$$

The last interval B_t is the backward recurrence time, or the age of the resetting process at time t , i.e., the elapsed time since the last resetting event.

A realisation of the set of random variables $\mathbf{T}_1, \dots, \mathbf{T}_{M_t}, B_t$, with $M_t = m$, denoted by

$$\mathcal{C} = \{T_1, \dots, T_m, B\}, \quad (2.38)$$

has weight

$$P(\mathcal{C}) = f(T_1) \dots f(T_m) \Phi(B) \delta\left(\sum_{i=1}^m T_i + B, t\right). \quad (2.39)$$

Following the same approach as in (2.21), we have

$$Y(y, w) = \sum_{t \geq 0} w^t \langle y^{M_t} \rangle = \frac{\tilde{\Phi}(w)}{1 - y\tilde{f}(w)} = \frac{1}{1 - (1 - r + ry)w}. \quad (2.40)$$

Hence

$$\langle y^{M_t} \rangle = (1 - r + ry)^t, \quad (2.41)$$

implying that $M_t = 0, \dots, t$ has the binomial distribution

$$\mathbb{P}(M_t = m) = \binom{t}{m} r^m (1 - r)^{t-m} \quad (2.42)$$

at all times, in agreement with the property that resetting events are independent from each other, and therefore form a Bernoulli process. In particular, the mean number of resettings reads

$$\langle M_t \rangle = rt. \quad (2.43)$$

3 Spontaneous returns to the origin and resetting events

3.1 The key equation

As stated in the introduction, the main purpose of this work is to analyse the joint distribution of the numbers \mathcal{N}_t^\bullet of dots representing resetting events and \mathcal{N}_t^\times of crosses representing spontaneous returns to the origin, for the reset Pólya walk up to time t . These numbers are respectively given by

$$\mathcal{N}_t^\bullet = M_t, \quad (3.1)$$

introduced above, and

$$\mathcal{N}_t^\times = N_{T_1-1} + N_{T_2-1} + \dots + N_{T_{M_t-1}} + N_{B_t}, \quad (3.2)$$

as illustrated on figure 1. The sum of these two numbers is denoted by

$$\mathcal{N}_t^{\times\bullet} = \mathcal{N}_t^\times + \mathcal{N}_t^\bullet, \quad (3.3)$$

and reads

$$\mathcal{N}_t^{\times\bullet} = \sum_{\tau=1}^t \delta(x_\tau, 0), \quad (3.4)$$

where x_τ is the position of the walker at time τ (see (1.1)). This is the total time spent by the walker the origin, either by a resetting event (a dot) or by a spontaneous return (a cross).

Notice that the distribution of the number of dots, $\mathcal{N}_t^\bullet = M_t$ (see (3.1)), is known from (2.40), (2.41), (2.42) and (2.43). Thus

$$\mathcal{Y}(y, w) = \sum_{t \geq 0} w^t \langle y^{\mathcal{N}_t^\bullet} \rangle = Y(y, w) = \frac{1}{1 - (1 - r + ry)w}, \quad (3.5)$$

$$\langle y^{\mathcal{N}_t^\bullet} \rangle = (1 - r + ry)^t, \quad (3.6)$$

$$\mathbb{P}(\mathcal{N}_t^\bullet = \mathcal{N}) = \binom{t}{\mathcal{N}} r^{\mathcal{N}} (1 - r)^{t - \mathcal{N}}, \quad (3.7)$$

$$\langle \mathcal{N}_t^\bullet \rangle = rt. \quad (3.8)$$

Notice also that the situation simplifies in the following two special cases. First, in the absence of resetting ($r = 0$), we have

$$\mathcal{N}_t^\times = \mathcal{N}_t^{\times \bullet} = N_t, \quad \mathcal{N}_t^\bullet = 0, \quad (3.9)$$

second, when a resetting event occurs at every time step ($r = 1$), then

$$\mathcal{N}_t^\bullet = \mathcal{N}_t^{\times \bullet} = t, \quad \mathcal{N}_t^\times = 0. \quad (3.10)$$

The central quantity for the determination of the joint statistics of \mathcal{N}_t^\times and \mathcal{N}_t^\bullet is the generating function

$$\mathcal{Z}(z, y, t) = \langle z^{\mathcal{N}_t^\times} y^{\mathcal{N}_t^\bullet} \rangle, \quad (3.11)$$

where the average is taken over the external configurations \mathcal{C} (see (2.38)), with weight $P(\mathcal{C})$ given by (2.39), and over the internal configurations $\tilde{\mathcal{C}}$ (see (2.15)), with weight $P(\tilde{\mathcal{C}})$ given by (2.16). Thus

$$\mathcal{Z}(z, y, t) = \sum_{\mathcal{C}} P(\mathcal{C}) \sum_{\tilde{\mathcal{C}}} P(\tilde{\mathcal{C}}) z^{\mathcal{N}_t^\times} y^{\mathcal{N}_t^\bullet}, \quad (3.12)$$

with the notations

$$\sum_{\mathcal{C}} = \sum_{m \geq 0} \sum_{\{T_i, B\}}, \quad \sum_{\tilde{\mathcal{C}}} = \sum_{n \geq 0} \sum_{\{\tau_i, b\}}. \quad (3.13)$$

The average over the internal variables of each term $z^{\mathcal{N}_t^\times} y^{\mathcal{N}_t^\bullet}$ with weight $P(\tilde{\mathcal{C}})$ gives a factor $Z(z, T_i - 1)$ (see (2.19)). We then average over the external variables with weight $P(\mathcal{C})$ to arrive at

$$\langle z^{\mathcal{N}_t^\times} y^{\mathcal{N}_t^\bullet} \rangle = \sum_{\mathcal{C}} P(\mathcal{C}) y^m Z(z, T_1 - 1) \dots Z(z, T_m - 1) Z(z, B). \quad (3.14)$$

The expression thus obtained is a discrete convolution, which is easier to handle by taking its generating function with respect to t , leading to

$$\tilde{Z}(z, y, w) = \sum_{t \geq 0} w^t Z(z, y, t) = \sum_{m \geq 0} y^m \tilde{\varphi}(z, w)^m \tilde{\psi}(z, w) = \frac{\tilde{\psi}(z, w)}{1 - y \tilde{\varphi}(z, w)}, \quad (3.15)$$

with

$$\tilde{\varphi}(z, w) = \sum_{T \geq 1} w^T f(T) Z(z, T - 1), \quad (3.16)$$

$$\tilde{\psi}(z, w) = \sum_{B \geq 0} w^B \Phi(B) Z(z, B). \quad (3.17)$$

The expressions (3.15)–(3.17) are quite general [1]. They hold for arbitrary distributions $\rho(\tau)$ and $f(T)$, both in a continuous and in a discrete setting. For the case at hand, the generating functions of $Z(z, T)$, $f(T)$ and $\Phi(T)$ are respectively given in (2.21), (2.34) and (2.35). We have therefore

$$\begin{aligned} \tilde{\varphi}(z, w) &= rw \tilde{Z}(z, \check{w}), \\ \tilde{\psi}(z, w) &= \tilde{Z}(z, \check{w}), \end{aligned} \quad (3.18)$$

where we introduced the shorthand notation

$$\check{w} = (1 - r)w, \quad (3.19)$$

and finally

$$\tilde{Z}(z, y, w) = \frac{\tilde{Z}(z, \check{w})}{1 - ryw \tilde{Z}(z, \check{w})}. \quad (3.20)$$

The expression (3.20), where $\tilde{Z}(z, w)$ is given in (2.21), and $\tilde{\rho}(w)$ in (2.2), is the key result of this section.

The distribution of $\mathcal{N}_t^\bullet = M_t$ is obtained by setting $z = 1$ in (3.20). We thus recover the expression (3.5), since $\tilde{Z}(1, y, w) = \mathcal{Y}(y, w)$, as it should be. The distribution of \mathcal{N}_t^\times is obtained by setting $y = 1$ in (3.20). We thus have

$$\tilde{Z}(z, 1, w) = \sum_{t \geq 0} w^t \langle z^{\mathcal{N}_t^\times} \rangle = \frac{\tilde{Z}(z, \check{w})}{1 - rw \tilde{Z}(z, \check{w})}. \quad (3.21)$$

This formula relates the same quantity with and without resetting. Rational relationships of this form are specific to Poissonian resetting in continuous time or to geometric resetting in discrete time (see, e.g., [3–6, 11, 13]). Another interpretation of (3.21) will be given in section 3.2.

The general expression of the mean value $\langle \mathcal{N}_t^\times \rangle$ ensues from (3.15), and reads

$$\sum_{t \geq 0} w^t \langle \mathcal{N}_t^\times \rangle = \frac{d}{dz} \mathcal{Z}(z, y, w) \Big|_{z=y=1} \quad (3.22)$$

$$= \frac{1}{1 - \tilde{f}(w)} \left(\sum_{T \geq 1} w^T \langle N_{T-1} \rangle \frac{f(T)}{1-w} + \sum_{B \geq 0} w^B \langle N_B \rangle \Phi(B) \right). \quad (3.23)$$

In the case at hand, this expression yields

$$\sum_{t \geq 0} w^t \langle \mathcal{N}_t^\times \rangle = \frac{(1 - \tilde{w}) \tilde{\rho}(\tilde{w})}{(1 - w)^2 (1 - \tilde{\rho}(\tilde{w}))}, \quad (3.24)$$

which can alternatively be obtained from (3.20).

In the absence of resetting ($r = 0$), (3.24) gives back (2.22), as it should be, since $\mathcal{N}_t^\times = N_t$. In the presence of resetting ($r \neq 0$), we obtain the linear growth law

$$\langle \mathcal{N}_t^\times \rangle \approx A^\times t \quad (3.25)$$

in the late-time regime, with

$$A^\times = \frac{r \tilde{\rho}(1-r)}{1 - \tilde{\rho}(1-r)} = \sqrt{\frac{r}{2-r}} - r. \quad (3.26)$$

In the regime of weak resetting, the mean value $\langle \mathcal{N}_t^\times \rangle$ exhibits a smooth crossover between the square-root law (2.25) and the linear law (3.25). The complete determination of the distribution of \mathcal{N}_t^\times throughout this crossover regime will be given in section 5.

Summing expressions (3.8) and (3.25), we end up with

$$\langle \mathcal{N}_t^{\times \bullet} \rangle \approx At, \quad (3.27)$$

with

$$A = \sqrt{\frac{r}{2-r}}. \quad (3.28)$$

Both amplitudes A^\times and A vanish as

$$A^\times \approx A \approx \sqrt{\frac{r}{2}} \quad (3.29)$$

as $r \rightarrow 0$. This square-root scaling will be corroborated by the analysis of the crossover regime (see section 5). The amplitude A^\times vanishes quadratically as

$$A^\times \approx \frac{(1-r)^2}{2} \quad (3.30)$$

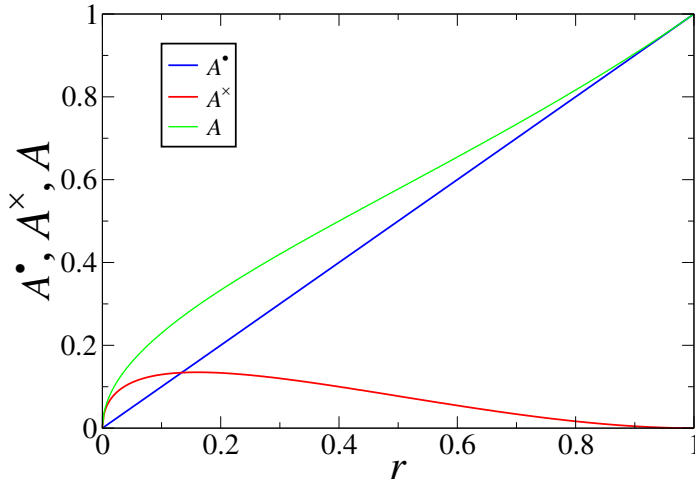


Fig. 3 Amplitudes $A^\bullet = r$, A^\times and their sum A entering the growth laws (3.8), (3.25) and (3.27) of $\langle \mathcal{N}_t^\bullet \rangle$, $\langle \mathcal{N}_t^\times \rangle$ and $\langle \mathcal{N}_t^{\times\bullet} \rangle$, plotted against the resetting probability r .

as $r \rightarrow 1$, testifying that the presence of a cross, i.e., of a spontaneous return of the walker to the origin, requires at least two successive time steps without resetting. This amplitude reaches its maximum $A_{\max}^\times = 0.134884\dots$ for $r = 0.160713\dots$. As for the amplitude A of $\langle \mathcal{N}_t^{\times\bullet} \rangle$, it increases monotonically from 0 to 1 as r increases in the same range of values. Figure 3 shows plots of the amplitudes $A^\bullet = r$, A^\times , and of their sum A , against the resetting probability r .

The formula (3.28) can be compared with the expression derived in [6] for the position distribution of the walker in the nonequilibrium stationary state reached in the limit of infinitely large times, namely

$$p(x) = \sqrt{\frac{r}{2-r}} \lambda^{-|x|}, \quad \lambda = \frac{1 + \sqrt{r(2-r)}}{1-r}. \quad (3.31)$$

This distribution falls off exponentially with the distance to the resetting point, i.e., the origin, where it reaches its maximum

$$p(0) = \sqrt{\frac{r}{2-r}}. \quad (3.32)$$

The identity $A = p(0)$ is to be expected, as both sides represent the fraction of time spent by the walker at the origin. Formally, this identity can be derived by taking the mean values of (3.4) and using the fact that the occupation probability of the origin at time t , $\langle \delta(x_t, 0) \rangle$, tends to $p(0)$ at late times.

3.2 The reset process seen as a ‘dressed’ renewal process

It is interesting to note that there exists another interpretation of the expression (3.21), encoding the full statistics of \mathcal{N}_t^\times . This expression is of the form (2.21), up to the

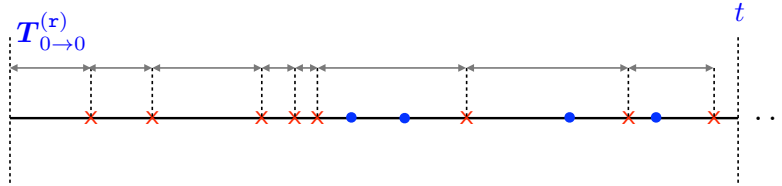


Fig. 4 The time intervals between spontaneous returns to the origin (crosses) of the reset random walk form a renewal process, described in terms of the ‘dressed’ probability distribution (3.34). These time intervals are probabilistic copies of the first one, $\mathbf{T}_{0 \rightarrow 0}^{(x)}$, the ‘dressed’ first-passage time. (Compare to figure 2.)

replacement of $\tilde{\rho}(w)$ by

$$\tilde{\rho}^{(x)}(w) = \frac{(1 - \check{w})\tilde{\rho}(\check{w})}{1 - w + rw\tilde{\rho}(\check{w})}. \quad (3.33)$$

This implies that the interarrival times between spontaneous returns to the origin (crosses in figure 2) remain, in the presence of resetting, independent, identically distributed, random variables, whose common probability distribution,

$$\rho^{(x)}(\tau) = \mathbb{P}(\mathbf{T}_{0 \rightarrow 0}^{(x)} = \tau), \quad (3.34)$$

has a generating function given by (3.33), and depends only on the resetting probability r (see (3.35)). In other words, these interarrival times form a renewal process, defined by the ‘dressed’ distribution (3.34), i.e., they are probabilistic replicas of the ‘dressed’ first-passage time $\mathbf{T}_{0 \rightarrow 0}^{(x)}$ (or, in the present context, time of first return to the origin), as depicted in figure 4. The superscript in these expressions is an abbreviation for *replication* or *resetting*.

The first few values of $\rho^{(x)}(\tau)$ read

$$\begin{aligned} \rho^{(x)}(1) &= 0, & \rho^{(x)}(2) &= \frac{1}{2}(1 - r)^2, & \rho^{(x)}(3) &= \frac{1}{2}r(1 - r)^2, \\ \rho^{(x)}(4) &= \frac{1}{8}(1 - r)^4 + \frac{1}{2}r^2(1 - r)^2 + \frac{1}{2}r(1 - r)^3 = \frac{1}{8}(1 - r^2)^2. \end{aligned} \quad (3.35)$$

The first three expressions are easy to guess, whereas the fourth is the sum of the probabilities of the following events: {return to the origin in four steps without any resetting}, {two resettings first, then return to the origin in two steps}, and finally {one step away from the origin, a resetting, then return to the origin in two steps}. The right-hand sides in (3.35) give back (2.6), when $r = 0$.

The existence of the aforementioned dressed renewal process is a remarkable phenomenon, which occurs whether the time intervals between resetting events, pertaining to the external renewal process, follow an exponential distribution in continuous time (resulting in a Poisson process), as described in [1], or a geometric distribution (see (2.32)) in discrete time (resulting in a Bernoulli process), as described above. This allows us to access several characteristic features of the reset Pólya walk by considering quantities pertaining to the dressed renewal process, as we now elaborate.

The ‘dressed’ survival probability is naturally defined, in line with (2.8), as

$$R^{(x)}(\tau) = \mathbb{P}(\mathbf{T}_{0 \rightarrow 0}^{(x)} > \tau) = \sum_{j > \tau} \rho^{(x)}(j). \quad (3.36)$$

Starting from (3.33) and using (2.9), as well as the corresponding generating function for the dressed distribution,

$$\tilde{R}^{(x)}(w) = \frac{1 - \tilde{\rho}^{(x)}(w)}{1 - w}, \quad (3.37)$$

we can establish the following connection between the generating functions for the survival probabilities (2.8) and (3.36) in the absence or in the presence of resetting,

$$\tilde{R}^{(x)}(w) = \frac{\tilde{R}(\check{w})}{1 - rw\tilde{R}(\check{w})}. \quad (3.38)$$

The same relation holds for the probability of not crossing the origin up to integer time t , for a discrete-time walker with continuous steps [4], or for the Pólya walk [13].

The moments of $\mathbf{T}_{0 \rightarrow 0}^{(x)}$ can be derived from (3.33). We have in particular

$$\langle \mathbf{T}_{0 \rightarrow 0}^{(x)} \rangle = \frac{1}{A^\times}, \quad (3.39)$$

meaning that $\langle \mathbf{T}_{0 \rightarrow 0}^{(x)} \rangle$ has a minimum at $r = 0.160713\dots$, and that (3.25) can be recast as

$$\langle \mathcal{N}_t^\times \rangle \approx \frac{t}{\langle \mathbf{T}_{0 \rightarrow 0}^{(x)} \rangle}, \quad (3.40)$$

which is consistent with intuition.

Another quantity of interest is the probability of occurrence of a cross (spontaneous return to the origin of the Pólya walk) at time t , in the absence or in the presence of resetting, i.e., respectively,

$$U(t) = \langle N_t \rangle - \langle N_{t-1} \rangle, \quad U^{(x)}(t) = \langle \mathcal{N}_t^\times \rangle - \langle \mathcal{N}_{t-1}^\times \rangle \quad (t \geq 1), \quad (3.41)$$

completed by $U(0) = U^{(x)}(0) = 1$. The corresponding generating functions are given by (see (2.22))

$$\tilde{U}(w) = \frac{1}{1 - \tilde{\rho}(w)}, \quad \tilde{U}^{(x)}(w) = \frac{1}{1 - \tilde{\rho}^{(x)}(w)}. \quad (3.42)$$

We have $U(2n) = b_n$ (see (2.3)), whereas $U(2n+1) = 0$. For t large, $U^{(x)}(t)$ converges very rapidly to A^\times . The expression of $U^{(x)}(t)$ in the crossover regime of weak resetting and late times will be given in (5.22).

The tail of the dressed distribution $\rho^{(x)}(\tau)$ falls off exponentially as

$$\rho^{(x)}(\tau) \sim e^{-\sigma\tau}. \quad (3.43)$$

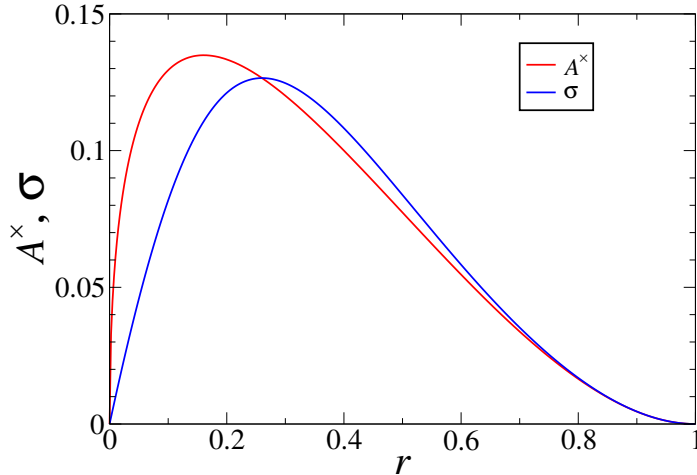


Fig. 5 Amplitude A^\times (see (3.25) and (3.39)) and decay rate σ (see (3.43)), plotted against the resetting probability r .

The decay rate σ is such that $w_0 = e^\sigma$ is the smallest zero of the denominator of (3.33), obeying

$$r^2(1-r)w_0^3 + r^2w_0^2 + (1-r)w_0 - 1 = 0. \quad (3.44)$$

The dependence of the decay rate σ on r is qualitatively similar to that of the amplitude A^\times (see figure 5). It vanishes as $\sigma \approx r$ as $r \rightarrow 0$, and as $\sigma \approx (1-r)^2/2$ as $r \rightarrow 1$ (compare to (3.29) and (3.30)), reaching its maximum $\sigma_{\max} = 0.126530\dots$ for $r = 0.260465\dots$

As a summary, while the original renewal process made of the spontaneous returns to the origin of the Pólya walk is not stationary, since the distribution (2.7) has a fat power-law tail, the dressed renewal process defined by the exponentially decaying distribution (3.43) becomes eventually stationary (see [1, 16]).

The formula (3.33) is presented in [11] within a different context. It appears as an application to geometric resetting of a general formula concerning the distribution of first-passage times in a generic discrete-step walk in the presence of an arbitrary distribution of reset events. This reference solely focuses on first-passage properties. In particular, it does not delve into the renewal structure of the spontaneous returns to the origin of the reset Pólya walk defined by (1.1). The method used in [11] to derive the distribution of the first-passage time for an arbitrary distribution of reset events, which builds upon prior research [10, 17, 18], is revisited in [1].

4 Cumulants and large deviations in the late-time regime

In this section we continue the investigation of the joint statistics of the quantities \mathcal{N}_t^\times (number of dots) and \mathcal{N}_t^\bullet (number of crosses) for the Pólya walk in the late-time regime. We shall demonstrate that these variables are extensive in a strong sense, first

by examining their joint cumulants and then by investigating the corresponding large deviation functions.

4.1 Cumulants

The starting point of the analysis is again the key formula (3.20). The late-time regime is governed by the smallest zero $w_*(z, y)$ of the denominator of that formula, which entails an exponential law of the form

$$\langle z^{\mathcal{N}_t^\times} y^{\mathcal{N}_t^\bullet} \rangle \sim w_*(z, y)^{-t} \quad (4.1)$$

for the joint probability generating function of \mathcal{N}_t^\times and \mathcal{N}_t^\bullet in the late-time regime. Introducing the notations

$$z = e^\lambda, \quad y = e^\mu, \quad (4.2)$$

and

$$w_*(z, y) = e^{-S(\lambda, \mu)} \quad (4.3)$$

brings the estimate (4.1) for the generating function of the joint cumulants of \mathcal{N}_t^\times and \mathcal{N}_t^\bullet to the more familiar form

$$\langle e^{\lambda \mathcal{N}_t^\times + \mu \mathcal{N}_t^\bullet} \rangle \sim e^{S(\lambda, \mu)t}. \quad (4.4)$$

The exponential law (4.4) implies that all joint cumulants grow linearly with time, as

$$\langle (\mathcal{N}_t^\times)^k (\mathcal{N}_t^\bullet)^\ell \rangle_c \approx c_{k, \ell} t, \quad (4.5)$$

where the amplitudes $c_{k, \ell}$ are the coefficients of the series expansion

$$S(\lambda, \mu) = \sum_{k+\ell \geq 1} c_{k, \ell} \frac{\lambda^k}{k!} \frac{\mu^\ell}{\ell!} \quad (4.6)$$

of the entropy function $S(\lambda, \mu)$ entering (4.4).

In particular, setting $\lambda = \mu$ in (4.4) yields

$$\langle e^{\lambda \mathcal{N}_t^{\times \bullet}} \rangle \sim e^{S(\lambda, \lambda)t}, \quad (4.7)$$

so that $S(\lambda, \lambda)$ generates the amplitudes of the cumulants of $\mathcal{N}_t^{\times \bullet} = \mathcal{N}_t^\times + \mathcal{N}_t^\bullet$ in the late-time regime. We have

$$\langle (\mathcal{N}_t^{\times \bullet})^n \rangle_c \approx C_n t, \quad (4.8)$$

with

$$S(\lambda, \lambda) = \sum_{n \geq 1} C_n \frac{\lambda^n}{n!} \quad (4.9)$$

and

$$C_n = \sum_{k=0}^n \binom{n}{k} c_{k, n-k}. \quad (4.10)$$

In order to derive explicit expressions for the function $S(\lambda, \mu)$ defined in (4.3), and therefore for the cumulant amplitudes $c_{k,\ell}$ and C_n , we need an expression of the smallest zero of the denominator in (3.20). This is done in Appendix A, yielding $w_*(z, y) = w_1$, where w_1 is known explicitly from (4.2), (A2), (A4), (A5) and (A6), whence, finally,

$$S(\lambda, \mu) = -\ln w_1. \quad (4.11)$$

By expanding the expression above as a power series in λ and μ , we obtain explicit expressions for the cumulants $c_{k,\ell}$ and C_n , which can be further reduced to expressions linear in

$$A = \sqrt{\frac{r}{2-r}} \quad (4.12)$$

(see (3.28)), with coefficients rational in r . The first few formulas given below testify that their complexity increases very fast with the order of the cumulants. To first order in λ and μ , we have

$$\begin{aligned} c_{1,0} &= A - r, \\ c_{0,1} &= r, \\ C_1 &= A, \end{aligned} \quad (4.13)$$

in agreement with (3.8), (3.26) and (3.28). To second order, we have

$$\begin{aligned} c_{2,0} &= -\frac{4-3r}{2-r}A + \frac{2+4r-9r^2+5r^3-r^4}{(2-r)^2}, \\ c_{1,1} &= \frac{1-r}{2-r}A - r(1-r), \\ c_{0,2} &= r(1-r), \\ C_2 &= -A + \frac{2-r^2}{(2-r)^2}. \end{aligned} \quad (4.14)$$

To third order, we have

$$\begin{aligned} c_{3,0} &= \frac{3+38r-76r^2+46r^3-8r^4}{r(2-r)^3}A \\ &\quad - \frac{12+14r-66r^2+73r^3-43r^4+15r^5-2r^6}{(2-r)^3}, \\ c_{2,1} &= -\frac{(1-r)(4-5r)}{(2-r)^2}A \\ &\quad + \frac{r(1-r)(12-32r+30r^2-13r^3+2r^4)}{(2-r)^3}, \\ c_{1,2} &= \frac{(1-r)(1-2r)}{(2-r)^2}A - r(1-r)(1-2r), \\ c_{0,3} &= r(1-r)(1-2r), \end{aligned}$$

$$C_3 = \frac{3 + 20r - 31r^2 + 10r^3 + r^4}{r(2-r)^3} A - \frac{3(2-r^2)}{(2-r)^2}. \quad (4.15)$$

More specific results can be derived in a few special and limiting situations. We have observed that the statistics of \mathcal{N}_t^\bullet is simple, as its distribution is the binomial (3.7). This leads to two consequences. First, all its cumulants have an exact linear behaviour in t at all times:

$$\langle (\mathcal{N}_t^\bullet)^\ell \rangle_c = c_{0,\ell} t. \quad (4.16)$$

Second, the cumulant amplitudes $c_{0,\ell}$ can be derived from (3.6), which amounts to

$$S(0, \mu) = \sum_{\ell \geq 1} c_{0,\ell} \frac{\mu^\ell}{\ell!} = \ln(1 - r + re^\mu). \quad (4.17)$$

The first few amplitudes read

$$\begin{aligned} c_{0,1} &= r, & c_{0,2} &= r(1-r), \\ c_{0,3} &= r(1-r)(1-2r), & c_{0,4} &= r(1-r)(1-6r+6r^2). \end{aligned} \quad (4.18)$$

The first three expressions agree with (4.13)–(4.15). The amplitudes $c_{0,\ell}$ are polynomials in r of increasing degrees, obeying the linear differential recursion [19]

$$c_{0,\ell+1} = r(1-r) \frac{dc_{0,\ell}}{dr} \quad (\ell \geq 1). \quad (4.19)$$

They read explicitly

$$c_{0,\ell} = \sum_{k=1}^{\ell} (-1)^{k-1} (k-1)! \left\{ \begin{matrix} \ell \\ k \end{matrix} \right\} r^k, \quad (4.20)$$

where $\left\{ \begin{matrix} \ell \\ k \end{matrix} \right\}$ are the Stirling numbers of the second kind.

In the regime of strong resetting ($r \rightarrow 1$), we have

$$S(\lambda, \mu) = \mu + (1-r)(e^{-\mu} - 1) + (1-r)^2(e^{-\mu} - e^{-2\mu} + \frac{1}{2}(e^{\lambda-2\mu} - 1)) + \dots \quad (4.21)$$

For $r = 1$, only $c_{0,1} = 1$ is non-zero, in agreement with (3.10). To first order in $1-r$, only the $c_{0,\ell}$ are non-zero, as there are no crosses at this order. Their behaviour $c_{0,\ell} \approx (-1)^\ell (1-r)$ for $\ell \geq 2$ agrees with (4.20). All cumulant amplitudes $c_{k,\ell}$ become non-trivial to second order in $1-r$.

The regime of weak resetting ($r \rightarrow 0$) is more subtle. This richness is related to the crossover phenomenon that will be examined in section 5. An inspection of the formulas (4.13), (4.14) and (4.15) yields the scaling $c_{k,\ell} \sim A^{2-k}$, with $A \approx \sqrt{r/2}$ (see (3.28)), at least for odd k . This observation can be corroborated by the following scaling analysis. Let us assume that the cumulant amplitudes behave as

$$c_{k,\ell} \approx b_{k,\ell} A^{2-k} \quad (4.22)$$

as $A \rightarrow 0$, i.e., $r \rightarrow 0$, where the $b_{k,\ell}$ are constants to be determined. This ansatz translates into the scaling form

$$S(\lambda, \mu) \approx A^2 F(h, \mu), \quad (4.23)$$

with

$$h = \frac{\lambda}{A}, \quad F(h, \mu) = \sum_{k+\ell \geq 1} b_{k,\ell} \frac{h^k}{k!} \frac{\mu^\ell}{\ell!}. \quad (4.24)$$

Inserting the scaling form (4.23), with the notations (4.2), into (A1), and expanding to the first non-trivial order in A , we obtain that the scaling function $F(h, \mu)$ obeys the quadratic equation

$$2F^2 - (8(e^\mu - 1) + h^2)F + 8(e^\mu - 1)^2 - 2h^2 = 0, \quad (4.25)$$

hence

$$F(h, \mu) = 2(e^\mu - 1) + \frac{h^2}{4} + h\sqrt{e^\mu + \frac{h^2}{16}}. \quad (4.26)$$

Each term of the expression (4.26) is responsible for the scaling (4.22) of some of the cumulant amplitudes as $A \rightarrow 0$. The first term yields

$$c_{0,\ell} \approx 2A^2 \approx r \quad (4.27)$$

for all $\ell \geq 1$, in agreement with (4.20). The second term yields

$$c_{2,0} \rightarrow \frac{1}{2} \quad (4.28)$$

as $r \rightarrow 0$, in agreement with (4.14). The third term of (4.26) is an odd function of h , and therefore concerns odd values of k . Introducing the series expansion

$$\sqrt{1 + \frac{x}{16}} = \sum_{p \geq 0} \frac{a_p}{(2p+1)!} x^p, \quad a_p = (-1)^{p-1} \frac{(2p+1)!}{16^p(2p-1)} b_p \quad (4.29)$$

(see (2.3)), i.e.,

$$a_0 = 1, \quad a_1 = \frac{3}{16}, \quad a_2 = -\frac{15}{256}, \quad a_3 = \frac{315}{4096}, \quad (4.30)$$

and so on, we obtain

$$c_{2p+1,\ell} \approx a_p \left(-\frac{1}{2}(2p-1)\right)^\ell A^{1-2p}. \quad (4.31)$$

All cumulant amplitudes $c_{k,\ell}$ with odd k therefore obey the scaling ansatz (4.22), while the cumulant amplitudes with even k are subleading as $r \rightarrow 0$, with the exception of those previously mentioned in (4.27) and (4.28). Finally, the cumulant amplitudes C_n for odd n are governed by the term $k = n$ in (4.10). We have therefore

$$C_{2p+1} \approx a_p A^{1-2p}, \quad (4.32)$$

whereas the C_n with even n are subleading as $r \rightarrow 0$, except $C_2 \approx c_{2,0} \approx 1/2$.

4.2 Large deviations

The result (4.4) has an alternative interpretation in terms of large deviations [20–23]. It implies that the joint probability distribution of \mathcal{N}_t^\times and \mathcal{N}_t^\bullet falls off exponentially as

$$\mathbb{P}(\mathcal{N}_t^\times \approx \xi t, \mathcal{N}_t^\bullet \approx \eta t) \sim e^{-I(\xi, \eta)t} \quad (4.33)$$

in the regime of late times, for fixed densities ξ of crosses and η of dots. The estimate

$$\langle e^{\lambda \mathcal{N}_t^\times + \mu \mathcal{N}_t^\bullet} \rangle \sim \int d\xi \int d\eta e^{[\lambda \xi + \mu \eta - I(\xi, \eta)]t} \sim e^{S(\lambda, \mu)t} \quad (4.34)$$

shows that the bivariate functions $S(\lambda, \mu)$ and $I(\xi, \eta)$ are related by a Legendre transformation of the form

$$S(\lambda, \mu) + I(\xi, \eta) = \lambda \xi + \mu \eta, \quad (4.35)$$

with

$$\xi = \frac{\partial S}{\partial \lambda}, \quad \eta = \frac{\partial S}{\partial \mu}, \quad \lambda = \frac{\partial I}{\partial \xi}, \quad \mu = \frac{\partial I}{\partial \eta}. \quad (4.36)$$

In the late-time regime, the joint distribution of \mathcal{N}_t^\times and \mathcal{N}_t^\bullet becomes peaked around the point

$$\xi_0 = A^\times = A - r = c_{1,0}, \quad \eta_0 = A^\bullet = r = c_{0,1}, \quad (4.37)$$

in agreement with (3.8), (3.25) and (4.13). The form of the bivariate large deviation function $I(\xi, \eta)$ around (ξ_0, η_0) is governed by the regime where λ and μ are small. Using the series expansion (4.6), we are left with the quadratic form (see (4.14))

$$I(\xi, \eta) \approx \frac{c_{0,2}(\xi - \xi_0)^2 - 2c_{1,1}(\xi - \xi_0)(\eta - \eta_0) + c_{2,0}(\eta - \eta_0)^2}{2(c_{2,0}c_{0,2} - c_{1,1}^2)}, \quad (4.38)$$

describing the Gaussian bulk of the joint distribution of \mathcal{N}_t^\times and \mathcal{N}_t^\bullet .

The subsequent analysis shows that the domain of permitted values of the densities ξ and η is the triangle ABC shown in figure 6. The large deviation function $I(\xi, \eta)$ is continuous all along the boundary of the triangle. Its behaviour near the vertices and the edges of the triangle is governed by the regime where λ and/or μ are large, either positive or negative.

The vertex A = (0, 0) is reached for λ and $\mu \rightarrow -\infty$. We obtain $S(-\infty, -\infty) = \ln(1 - r)$, and so

$$I_A = I(0, 0) = -\ln(1 - r). \quad (4.39)$$

This can be interpreted as follows. Point A corresponds to the situation where the system is empty. The absence of resettings ($\eta = 0$) brings a weight $(1 - r)^t$. Given this condition, the probability of the system containing no crosses ($\xi = 0$) is $R(t)$

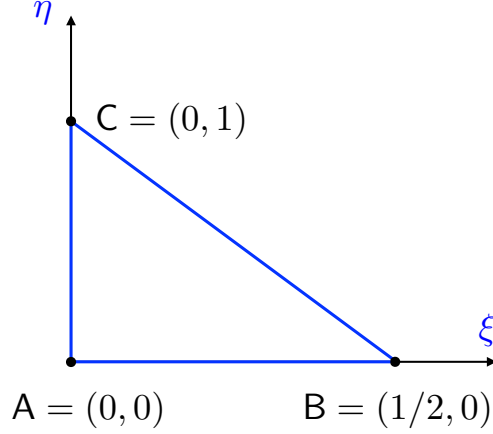


Fig. 6 Triangular domain of permitted values of densities ξ of returns to the origin of the walk (crosses) and η of resetting events (dots).

(see (2.27)), which falls off as a power of time (see (2.12)), and thus does not contribute to the large deviation function. The vertex $B = (1/2, 0)$ is reached for $\lambda \rightarrow -\infty$ and $\mu \rightarrow +\infty$. We obtain

$$I_B = I(1/2, 0) = -\ln(1-r) + \frac{1}{2} \ln 2. \quad (4.40)$$

The absence of resettings ($\eta = 0$) indeed again brings a weight $(1-r)^t$. Given this condition, when time t is even, the number \mathcal{N}_t^\times of crosses takes its maximal value $t/2$, and $\xi = 1/2$, if the walk consists of a sequence of $t/2$ back-and-forth excursions on either side of the origin. This constraint brings a weight $2^{-t/2}$. The vertex $C = (0, 1)$ is reached for $\lambda \rightarrow +\infty$ and $\mu \rightarrow -\infty$. We obtain

$$I_C = I(0, 1) = -\ln r. \quad (4.41)$$

The condition $\eta = 1$ indeed amounts to having a resetting event at each time step. This brings a weight r^t , and there is no space left for crosses.

Along the edge AB , $I(\xi, 0)$ increases monotonically from I_A to I_B . Along AC , $I(0, \eta)$ is not monotonic and exhibits a minimum, to be identified with $I^\times(0)$ (see below). Finally, a generic point along BC is reached for λ and $\mu \rightarrow +\infty$ in such a way that the difference $\lambda - 2\mu$ is kept fixed. The large deviation function thus obtained is not monotonic and exhibits a minimum.

Let us now turn to the univariate large deviation functions associated with \mathcal{N}_t^\bullet , \mathcal{N}_t^\times and their sum $\mathcal{N}_t^{\bullet \times}$. In the case of \mathcal{N}_t^\bullet , (4.33) yields

$$\mathbb{P}(\mathcal{N}_t^\bullet \approx \eta t) \sim e^{-I^\bullet(\eta)t} \quad (0 < \eta < 1), \quad (4.42)$$

where

$$I^\bullet(\eta) = \min_{\xi} I(\xi, \eta) = \mu\eta - S(0, \mu) \quad (4.43)$$

is the Legendre transform of the function $S(0, \mu)$ given in (4.17). We thus obtain the simple expression

$$I^\bullet(\eta) = \eta \ln \frac{\eta}{r} + (1 - \eta) \ln \frac{1 - \eta}{1 - r}, \quad (4.44)$$

with limit values

$$I^\bullet(0) = I_A, \quad I^\bullet(1) = I_C, \quad (4.45)$$

and a quadratic behaviour

$$I^\bullet(\eta) \approx \frac{(\eta - r)^2}{r(1 - r)} \quad (4.46)$$

around $\eta_0 = r$.

In the case of \mathcal{N}_t^\times , (4.33) yields

$$\mathbb{P}(\mathcal{N}_t^\times \approx \xi t) \sim e^{-I^\times(\xi)t} \quad (0 < \xi < 1/2), \quad (4.47)$$

where

$$I^\times(\xi) = \min_{\eta} I(\xi, \eta) = \lambda \xi - S(\lambda, 0) \quad (4.48)$$

is the Legendre transform of $S(\lambda, 0)$. This function has the limit value

$$I^\times(1/2) = I_B \quad (4.49)$$

and the quadratic behaviour

$$I^\times(\xi) \approx \frac{(\xi - A^\times)^2}{2c_{2,0}} \quad (4.50)$$

around $\xi_0 = A^\times = c_{1,0}$. The limit value $I^\times(0)$ is given by the decay rate of the distribution of $\mathbf{T}_{0 \rightarrow 0}^{(x)}$, introduced in (3.43),

$$I^\times(0) = \sigma, \quad (4.51)$$

since $\mathbb{P}(\mathcal{N}_t^\times = 0) = R^{(x)}(t) \sim e^{-\sigma t}$, according to (3.36).

Finally, in the case of $\mathcal{N}_t^{\times\bullet} = \mathcal{N}_t^\times + \mathcal{N}_t^\bullet$, (4.33) yields

$$\mathbb{P}(\mathcal{N}_t^{\times\bullet} \approx \varphi t) \sim e^{-I(\varphi)t} \quad (0 < \varphi < 1), \quad (4.52)$$

where

$$I(\varphi) = \min_{\xi} I(\xi, \varphi - \xi) = \lambda \varphi - S(\lambda, \lambda) \quad (4.53)$$

is the Legendre transform of $S(\lambda, \lambda)$. The limit values

$$I(0) = I_A, \quad I(1) = I_C, \quad (4.54)$$

coincide with (4.45). The function $I(\varphi)$ has the expected quadratic behaviour

$$I(\varphi) \approx \frac{(\varphi - A)^2}{2C_2} \quad (4.55)$$

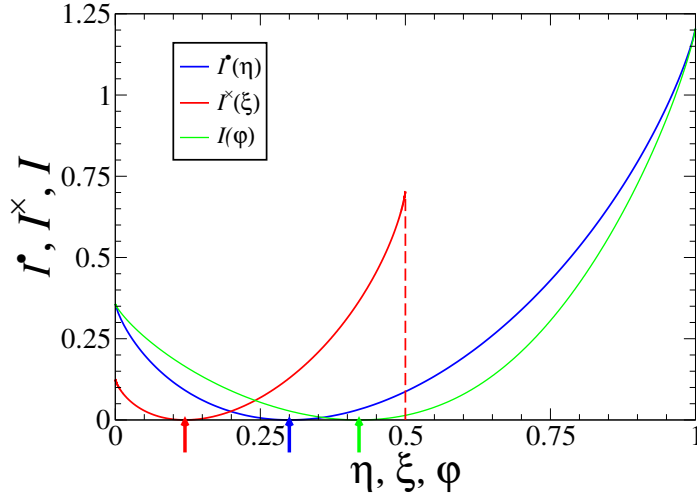


Fig. 7 Univariate large deviation functions $I^\bullet(\eta)$, $I^\times(\xi)$, and $I(\varphi)$, corresponding to \mathcal{N}_t^\bullet , \mathcal{N}_t^\times and their sum $\mathcal{N}_t^{\times\bullet}$, respectively, for a resetting probability $r = 0.3$, so that $\eta_0 = 0.3$, $\xi_0 = 0.120084\dots$ and $\varphi_0 = 0.420084\dots$ (arrows).

around $\varphi_0 = A = C_1$.

Figure 7 shows plots of the univariate large deviation functions $I^\bullet(\eta)$, $I^\times(\xi)$, and $I(\varphi)$, respectively corresponding to \mathcal{N}_t^\bullet , \mathcal{N}_t^\times and their sum $\mathcal{N}_t^{\times\bullet}$, for a resetting probability $r = 0.3$. Numerical values of these functions are obtained by means of (4.11). All derivatives required by the Legendre transform (4.35), (4.36) are worked out by analytical means. For instance,

$$\xi = \frac{\partial S}{\partial \lambda} = -\frac{\partial \ln w_1}{\partial \ln z} = -\frac{z}{w_1} \frac{\partial w_1}{\partial z} = \frac{z}{w} \frac{\partial P / \partial z}{\partial P / \partial w} \Big|_{w=w_1} \quad (4.56)$$

(see (A1)) is a rational expression in r , z , y and w_1 .

5 Crossover regime at weak resetting

The statistics of the number \mathcal{N}_t^\times of crosses exhibits a non-trivial behaviour in the crossover regime of weak resetting ($r \rightarrow 0$) and late times ($t \rightarrow \infty$). In the absence of resettings, the mean value $\langle \mathcal{N}_t^\times \rangle$ scales as \sqrt{t} (see (2.25)), while in the case of weak resetting, it scales as $\sqrt{r}t$ (see (3.25) and (3.26)). These two estimates become comparable when the product rt is of order unity. Interestingly, the latter is precisely the value of the mean number of resettings $\langle \mathcal{N}_t^\bullet \rangle$ (see (3.8)), which implies that a finite number of resetting events are sufficient to induce a macroscopic crossover in the statistics of \mathcal{N}_t^\times . This phenomenon has also been described in other observables, including the maximum and number of records of random walks under weak resetting [5, 6].

The full distribution of \mathcal{N}_t^\times throughout this crossover regime can be derived from (3.20). Setting $w = e^{-s}$, $y = 1$ and $z = e^{-p}$, and working to leading order in the

continuum regime where r , s and p are small, we obtain

$$\int_0^\infty dt e^{-st} \langle e^{-p\mathcal{N}_t^\times} \rangle \approx \frac{1}{s + p\sqrt{(r+s)/2}}. \quad (5.1)$$

Inverting the Laplace transform in p yields

$$\int_0^\infty dt e^{-st} \mathbb{P}(\mathcal{N}_t^\times = \mathcal{N}) \approx \sqrt{\frac{2}{r+s}} \exp\left(-s\sqrt{\frac{2}{r+s}}\mathcal{N}\right). \quad (5.2)$$

The two expressions above are very similar to (2.28) and (2.29). We thus infer from (5.2) that the number \mathcal{N}_t^\times of crosses scales as

$$\mathcal{N}_t^\times \approx \sqrt{t}\zeta, \quad (5.3)$$

where the rescaled random variable ζ has a limiting distribution with density $f(\zeta, u)$, depending only on the parameter

$$u = rt = \langle \mathcal{N}_t^\bullet \rangle. \quad (5.4)$$

Introducing the ratio $\lambda = s/r$, (5.2) becomes

$$f(\zeta, u) = \sqrt{2u} \int \frac{d\lambda}{2\pi i} \frac{e^{\lambda u}}{\sqrt{\lambda+1}} \exp\left(-\frac{\lambda}{\sqrt{\lambda+1}}\sqrt{2u}\zeta\right). \quad (5.5)$$

This expression cannot be made more explicit, except at $\zeta = 0$, resulting in the following value:

$$f(0, u) = \sqrt{2u} \int \frac{d\lambda}{2\pi i} \frac{e^{\lambda u}}{\sqrt{\lambda+1}} = \sqrt{\frac{2}{\pi}} e^{-u}. \quad (5.6)$$

Hereafter we examine the behaviour of this distribution in the regimes where the parameter u is either small or large. We then shift our focus to the analysis of the moments and the cumulants of ζ .

Behaviour for $u \ll 1$

The behaviour of $f(\zeta, u)$ for small u can be derived by setting $\lambda = p^2/u$ in (5.5), and expanding the integrand as a power series in u at fixed p . We thus obtain

$$\begin{aligned} f(\zeta, u) &= \int \frac{dp}{2\pi i} e^{p^2 - \sqrt{2}p\zeta} \left[2\sqrt{2} + \left(\frac{2\zeta}{p} - \frac{\sqrt{2}}{p^2} \right) u + \dots \right] \\ &= \sqrt{\frac{2}{\pi}} e^{-\zeta^2/2} + \left(2\zeta \operatorname{erfc} \frac{\zeta}{\sqrt{2}} - \sqrt{\frac{2}{\pi}} e^{-\zeta^2/2} \right) u + \dots, \end{aligned} \quad (5.7)$$

where erfc is the complementary error function. The first term matches the half-Gaussian asymptotic distribution (2.30) of \mathcal{N}_t^\times in the absence of resetting.

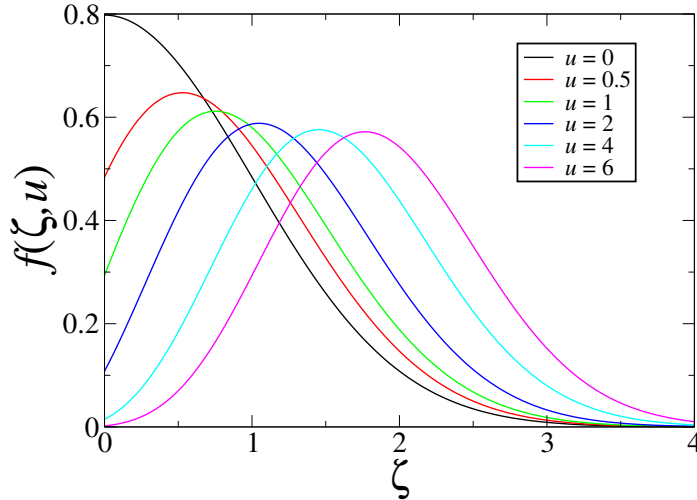


Fig. 8 Distribution $f(\zeta, u)$ of the rescaled number ζ of returns to the origin in the weak-resetting crossover regime (see (5.3)), for several values of the parameter $u = rt$ (see legend).

Behaviour for $u \gg 1$

Let us define the random variable X by

$$\zeta = \sqrt{\frac{u}{2}} + X. \quad (5.8)$$

The behaviour of $f(\zeta, u)$ for large u can then be derived by setting $\lambda = p/\sqrt{2u}$ in (5.5) and expanding the integrand as a power series in $1/\sqrt{u}$ at fixed p . We thus obtain, with $\zeta = \sqrt{u/2} + x$,

$$\begin{aligned} f(\zeta, u) &= \int \frac{dp}{2\pi i} e^{p^2/4 - px} \left(1 + \frac{8p^2x - 3p^3 - 8p}{16\sqrt{2u}} + \dots \right) \\ &= \frac{e^{-x^2}}{\sqrt{\pi}} \left(1 + \frac{x(2x^2 + 1)}{4\sqrt{2u}} + \dots \right). \end{aligned} \quad (5.9)$$

Whenever the parameter u is large, the random variable ζ therefore consists of a large deterministic part, growing as \sqrt{u} , along with a fluctuating component X of order unity. To leading order, the distribution of X is a Gaussian with variance $1/2$.

Figure 8 shows the distribution $f(\zeta, u)$ for several values of the parameter $u = rt$ (see legend). The plotted distributions exhibit a smooth but rather rapid crossover between a half-Gaussian form at $u = 0$ (see (5.7)) and a shifted Gaussian at large u (see (5.9)). In particular, the maxima of the curves converge very fast to their limit $1/\sqrt{\pi} = 0.564189\dots$

Moments of ζ

Equation (5.5) yields the following formula for the moments of ζ :

$$\mu_k(u) = \langle \zeta^k \rangle = \int_0^\infty d\zeta \zeta^k f(\zeta, u) = \frac{k!}{(2u)^{k/2}} \int \frac{d\lambda}{2\pi i} e^{\lambda u} \frac{(\lambda+1)^{k/2}}{\lambda^{k+1}}. \quad (5.10)$$

These moments only depend on the parameter $u = rt$. They are such that

$$\langle (\mathcal{N}_t^\times)^k \rangle \approx \mu_k(u) t^{k/2} \quad (5.11)$$

throughout the crossover regime. The moments (2.31) in the absence of resetting yield

$$\mu_{2n}(0) = \frac{(2n)!}{2^n n!}, \quad \mu_{2n+1}(0) = \sqrt{\frac{2}{\pi}} 2^n n!. \quad (5.12)$$

The results above suggest that the moments $\mu_k(u)$ have different analytical expressions according to the parity of the integer exponent k . This is indeed the case.

For even $k = 2n$, the integrand in the rightmost side of (5.10) is a rational function of λ . Expanding out $(\lambda+1)^n$, we readily obtain

$$\mu_{2n}(u) = \frac{(2n)!n!}{2^n} \sum_{m=0}^n \frac{u^m}{m!(n-m)!(n+m)!}, \quad (5.13)$$

namely

$$\mu_2(u) = \frac{u+2}{2}, \quad \mu_4(u) = \frac{u^2+8u+12}{4}, \quad \mu_6(u) = \frac{u^3+18u^2+90u+120}{8}, \quad (5.14)$$

and so on. The moment $\mu_{2n}(u)$ is a polynomial of degree n in u . Its constant term ($m=0$) matches the first expression in (5.12), whereas its leading term ($m=n$) yields

$$\mu_{2n}(u) \approx \left(\frac{u}{2}\right)^n, \quad (5.15)$$

in agreement with (5.8).

For odd $k = 2n+1$, the integrand in the rightmost side of (5.10) is now the ratio of a rational function by $\sqrt{\lambda+1}$. Proceeding as before, we obtain

$$\mu_{2n+1}(u) = \frac{(2n+1)!(n+1)!}{(2u)^{n+1/2}} \sum_{m=0}^{n+1} \frac{g_{n+m}(u)}{m!(n+1-m)!(n+m)!}, \quad (5.16)$$

with

$$g_n(u) = n! \int \frac{d\lambda}{2\pi i} \frac{e^{\lambda u}}{\lambda^{n+1} \sqrt{\lambda+1}} = \int_0^u dv (u-v)^n \frac{e^{-v}}{\sqrt{\pi v}}. \quad (5.17)$$

It can be shown using two integrations by parts that these functions obey the three-term linear recursion

$$g_n(u) = (u - n + \frac{1}{2})g_{n-1}(u) + (n-1)ug_{n-2}(u), \quad (5.18)$$

with initial values

$$g_0(u) = \operatorname{erf} \sqrt{u}, \quad g_1(u) = (u - \frac{1}{2}) \operatorname{erf} \sqrt{u} + \sqrt{\frac{u}{\pi}} e^{-u}. \quad (5.19)$$

We thus obtain

$$\begin{aligned} \mu_1(u) &= (2u+1) \frac{\operatorname{erf} \sqrt{u}}{2\sqrt{2u}} + \frac{e^{-u}}{\sqrt{2\pi}}, \\ \mu_3(u) &= (8u^3 + 36u^2 + 18u - 3) \frac{\operatorname{erf} \sqrt{u}}{16u\sqrt{2u}} + (4u^2 + 16u + 3) \frac{e^{-u}}{8u\sqrt{2\pi}}, \end{aligned} \quad (5.20)$$

and so on. The general structure of the odd moments emerges from the above examples. Their values at $u = 0$ (see (5.12)) cannot be easily read off, as more and more compensations are involved in taking the $u \rightarrow 0$ limit. To leading order at large u , we have

$$\mu_{2n+1}(u) \approx \left(\frac{u}{2}\right)^{n+1/2}, \quad (5.21)$$

again in agreement with (5.8).

To close, we mention that the probability $U^{(x)}(t)$ introduced in (3.41) scales as

$$U^{(x)}(t) \approx \frac{G(u)}{\sqrt{t}} \quad (5.22)$$

throughout the crossover regime, with

$$G(u) = \frac{1}{2}\mu_1(u) + u\mu_1'(u) = \frac{\sqrt{u} \operatorname{erf} \sqrt{u}}{\sqrt{2}} + \frac{e^{-u}}{\sqrt{2\pi}}. \quad (5.23)$$

The probability $U^{(x)}(t)$ exhibits even-odd oscillations, so that (5.22) actually describes the behaviour of the local average $\frac{1}{2}(U^{(x)}(t) + U^{(x)}(t-1))$.

Cumulants of ζ

In order to compare the above analysis of the crossover with the outcomes of section 4, let us consider the cumulants

$$\gamma_k(u) = \langle \zeta^k \rangle_c. \quad (5.24)$$

At large values of u , neglecting exponentially small corrections, these quantities read

$$\gamma_1(u) \approx \frac{2u+1}{2\sqrt{2u}}, \quad \gamma_2(u) \approx \frac{4u-1}{8u},$$

$$\begin{aligned}\gamma_3(u) &\approx \frac{6u-1}{16u\sqrt{2u}}, & \gamma_4(u) &\approx \frac{3}{32u^2}, \\ \gamma_5(u) &\approx -\frac{3(10u-3)}{128u^2\sqrt{2u}}, & \gamma_6(u) &\approx -\frac{15}{64u^3}.\end{aligned}\tag{5.25}$$

The cumulants of ζ appear to have a simpler dependence on u than the corresponding moments. To leading order as $u \gg 1$, the odd cumulants scale as

$$\gamma_{2n+1}(u) \approx a_n \left(\frac{u}{2}\right)^{1/2-n},\tag{5.26}$$

in agreement with (4.31), where the amplitudes a_n are given in (4.29). The second cumulant (variance) admits a finite limit $1/2$, to be identified with the limit of $c_{2,0}$, whereas higher even cumulants scale as

$$\gamma_{2n}(u) \approx \frac{\alpha_n}{u^n},\tag{5.27}$$

for some constants α_n . They are therefore subleading with respect to the odd ones.

6 Discussion

To conclude, let us put the main outcomes of the present work in perspective with those of the companion paper [1]. The point process considered in this latter work involves two generic nested renewal processes, an internal one characterised by the distribution $\rho(\tau)$ of interarrival times, and an external one characterised by the distribution $f(T)$ of time intervals between resetting events. In [1], the main emphasis was on the number \mathcal{N}_t^\times of (internal) renewal events occurring within a fixed observation time t . The statistics of this observable revealed a wide variety of asymptotic behaviours, dependent on the values of the exponents θ_1 and θ_2 governing the tails of the distributions $\rho(\tau)$ and $f(T)$. These findings highlight the dominance of the more regular of the two processes, specifically the one with the larger tail exponent, $\tilde{\theta} = \max(\theta_1, \theta_2)$. More specifically, \mathcal{N}_t^\times grows linearly in time and has relatively negligible fluctuations whenever $\tilde{\theta} > 1$, whereas $\mathcal{N}_t^\times \sim t^{\tilde{\theta}}$ grows subextensively over time while continuing to fluctuate for $\tilde{\theta} < 1$.

The reset Pólya walk considered in the present work is a specific instance of the general process made of two arbitrary nested renewal processes. The internal renewal process describes the spontaneous returns of the walker to its starting point, whereas the external one consists of resettings, taking place with probability r at each time step. In the phase diagram of [1], this example corresponds to $\theta_1 = 1/2$ and $\theta_2 = \infty$, and hence $\tilde{\theta} = \infty$, so that a high degree of regularity is expected for the entire process.

The present analysis corroborates this prediction and completes it by a breadth of quantitative results concerning the joint statistics of the numbers \mathcal{N}_t^\times of crosses (spontaneous returns) and \mathcal{N}_t^\bullet of dots (resetting events) in the regime of late times. The most salient of these outcomes—highlighted in the introduction—concerning the linear growth of all joint cumulants $\langle (\mathcal{N}_t^\times)^k (\mathcal{N}_t^\bullet)^\ell \rangle_c$ and the smoothness of the bivariate

large deviation function $I(\xi, \eta)$, testify that the numbers \mathcal{N}_t^\times and \mathcal{N}_t^\bullet are extensive in a very strong sense, and that the reset Pólya walk indeed manifests a very high degree of regularity. This characteristic can be related to the exponentially decaying, hence strongly localised, steady-state distribution of the walker's position under stochastic resetting (see (3.31)). It would be worth investigating whether similar regularity properties also manifest themselves in other observables pertaining to the Pólya walk under resetting.

Data availability statement

The authors have no data to share.

Conflict of interest

The authors declare no conflicts of interest.

Appendix A Zeros of the denominator of (3.20)

This appendix is devoted to the determination of the zeros of the denominator of (3.20) in the variable w . Using (2.21) and (2.2), and eliminating the square root entering the formula thus obtained, results in a polynomial equation of degree three for the zeros $w(z, y)$, reading

$$P(r, z, y, w) = P_3 w^3 + P_2 w^2 + P_1 w + P_0 = 0, \quad (\text{A1})$$

with

$$\begin{aligned} P_3 &= (1-r)((1-r)z + ry)^2, & P_2 &= r^2 y^2 - (1-r)^2 z^2, \\ P_1 &= (1-r)(1-2z) - 2ryz, & P_0 &= 2z - 1. \end{aligned} \quad (\text{A2})$$

Polynomial equations of degree three can be solved analytically, either by Cardano's method or by the trigonometric method. Here, we adopt the latter approach, which has the advantage that no complex numbers are involved when the three zeros are real. This is indeed the case here, for small enough real λ and μ . Setting $w = B + x$, we arrive at a reduced equation for x ,

$$x^3 + px + q = 0, \quad (\text{A3})$$

with

$$B = -\frac{P_2}{3P_3}, \quad p = \frac{P_1}{P_3} - \frac{P_2^2}{3P_3^2}, \quad q = \frac{P_0}{P_3} - \frac{P_1 P_2}{3P_3^2} + \frac{2P_2^3}{27P_3^3}. \quad (\text{A4})$$

The condition for all zeros to be real reads $4p^3 + 27q^2 < 0$, implying in particular $p < 0$. These zeros then read

$$\begin{aligned} w_1 &= B + \sigma \cos(\theta - 2\pi/3), \\ w_2 &= B + \sigma \cos \theta, \end{aligned}$$

$$w_3 = B + \sigma \cos(\theta + 2\pi/3), \quad (\text{A5})$$

with

$$\sigma = -\sqrt{-\frac{4p}{3}}, \quad \cos 3\theta = -\frac{4q}{\sigma^3} \quad (0 \leq \theta \leq \pi/3). \quad (\text{A6})$$

For small enough real λ and μ , the smallest of the three zeros is w_1 , which is positive, so that

$$S(\lambda, \mu) = -\ln w_1, \quad (\text{A7})$$

that is (4.11).

References

- [1] Godrèche, C., Luck, J.M.: Replicating a renewal process at random times. Preprint arXiv:2309.06997 (2023)
- [2] Pólya, G.: Über eine Aufgabe der Wahrscheinlichkeitsrechnung betreffend die Irrfahrt im Straßennetz. *Math. Annalen* **84**, 149–160 (1921)
- [3] Evans, M.R., Majumdar, S.N., Schehr, G.: Stochastic resetting and applications. *J. Phys. A: Math. Theor.* **53**, 193001 (2020)
- [4] Kusmierz, L., Majumdar, S.N., Sabhapandit, S., Schehr, G.: First order transition for the optimal search time of Lévy flights with resetting. *Phys. Rev. Lett.* **113**, 220602 (2014)
- [5] Majumdar, S.N., Mounaix, P., Sabhapandit, S., Schehr, G.: Record statistics for random walks and Lévy flights with resetting. *J. Phys. A: Math. Theor.* **55**, 034002 (2022)
- [6] Godrèche, C., Luck, J.M.: Maximum and records of random walks with stochastic resetting. *J. Stat. Mech.* **2022**, 063202 (2022)
- [7] Montero, M., Villarroel, J.: Directed random walk with random restarts: The Sisyphus random walk. *Phy. Rev. E* **94**, 032132 (2016)
- [8] Majumdar, S.N., Sabhapandit, S., Schehr, G.: Random walk with random resetting to the maximum position. *Phys. Rev. E* **92**, 052126 (2015)
- [9] Boyer, D., Solis-Salas, C.: Random walks with preferential relocations to places visited in the past and their application to biology. *Phys. Rev. Lett.* **112**, 240601 (2014)
- [10] Bonomo, O.L., Pal, A.: First passage under restart for discrete space and time: application to one-dimensional confined lattice random walks. *Phys. Rev. E* **103**, 052129 (2021)

- [11] Bonomo, O.L., Pal, A.: The Pólya and Sisyphus lattice random walks with resetting—a first passage under restart approach. Preprint arXiv:2106.14036 (2021)
- [12] Kumar, A., Pal, A.: Universal framework for record ages under restart. Phys. Rev. Lett. **130**, 157101 (2023)
- [13] Godrèche, C., Luck, J.M.: Survival probability of random walks and Lévy flights with stochastic resetting. J. Stat. Mech. **2022**, 073201 (2022)
- [14] Feller, W.: An Introduction to Probability Theory and Its Applications vol. 1. Wiley, New York (1968)
- [15] Feller, W.: An Introduction to Probability Theory and Its Applications vol. 2. Wiley, New York (1971)
- [16] Godrèche, C., Luck, J.M.: Statistics of the occupation time of renewal processes. J. Stat. Phys. **104**, 489–524 (2001)
- [17] Reuveni, S.: Optimal stochastic restart renders fluctuations in first passage times universal. Phys. Rev. Lett. **116**, 170601 (2016)
- [18] Pal, A., Reuveni, S.: First passage under restart. Phys. Rev. Lett. **118**, 030603 (2017)
- [19] Haldane, J.B.S.: The cumulants and moments of the binomial distribution, and the cumulants of χ^2 for a $(n \times 2)$ -fold table. Biometrika **31**, 392–396 (1940)
- [20] Ellis, R.S.: Entropy, Large Deviations, and Statistical Mechanics. Springer, New York (1985)
- [21] Dembo, A., Zeitouni, O.: Large Deviations Techniques and Applications. Springer, New York (2009)
- [22] Touchette, H.: The large deviation approach to statistical mechanics. Phys. Rep. **478**, 1–69 (2009)
- [23] Vulpiani, A., Cecconi, F., Cencini, M., Puglisi, A., Vergni, D.: Large Deviations in Physics: The Legacy of the Law of Large Numbers. Springer, New York (2014)